SPATIAL INTENSITY DISTRIBUTION OF WHISTLERS

Shinobu MACHIDA and Koichiro TSURUDA

Institute of Space and Astronautical Science,
6–1, Komaba 4-chome, Meguro-ku, Tokyo 153

***Abstract*:** The spatial intensity distribution of whistlers in the vicinity of the ionospheric wave exit region is investigated by analyzing the whistler data obtained at multiple stations. The typical attenuation gradient with the distance was derived to be 6 dB/100 km which was appreciably higher than what had been expected. A clear relationship between the attenuation gradient and the wave frequency was not found. The wave intensity peak on the ground took place at a higher latitude than that of the propagation path derived from the nose frequency of whistlers.

1. Introduction

The spatial distribution of VLF waves in the vicinity of the "wave exit region" from which the wave emerges into the free space was studied recently by TSURUDA *et al.* (1982), who analyzed the VLF waves transmitted from Siple Station and chorus emissions. They found that the VLF waves transmitted through the wave exit region showed an attenuation gradient as high as 6 dB/100 km along the earth's surface. This value is appreciably higher than that expected from previous theoretical work. WALKER (1974), for example, had calculated the horizontal attenuation rate for down-coming whistler-mode waves that couple with the earth-ionosphere cavity mode, and obtained a value of about 1.2 dB/100 km.

The location of the whistler duct can be derived by analyzing the nose frequency. However, this method can be applied neither to natural emissions which do not show definite frequency time characteristics nor to low latitude whistlers whose nose frequencies are above the frequency range usually received at ground station. As an alternative technique, several types of direction finding have been developed to locate the "wave exit region" from which the wave emerges into the free space (SAGREDO and BULLOUGH, 1973; LEAVITT, 1974; TSURUDA and HAYASHI, 1975; RYCROFT *et al.*, 1975; OKADA *et al.*, 1977; MATTHEWS *et al.*, 1979; TSURUDA and IKEDA, 1979; CARPENTER, 1980). RYCROFT *et al.* (1975) and MATTHEWS *et al.* (1979) compared whistler propagation paths drived from the nose frequency analysis and from the direction finder. Both authors have found that the L-values obtained by the direction finding are considerably lower than those determined by the nose frequency analysis. It is noted, however, that there exist some ambiguities in the determination of bearings by using the direction finding method. The wave bearings can be erroneous if two or more waves arrive at a receiver simultaneously, or if the size of the wave exit region is as large as a few hundred kilometers.

In this paper, we report on first the spatial attenuation rate of whistlers along the geomagnetic meridian and its dependence on wave frequency. Having confirmed that whistlers show high spatial attenuation rates we derive the location of the wave exit region from maxima in the spatial intensity distribution. This location is compared with the ionospheric foot of the whistler duct determined by the nose frequency analysis.

2. Outline of Experiment

Observations were made from July 10 to August 10, 1979 near Roberval, Canada. The locations of the stations D, E, F and G are shown in Fig. 1 and their geographic coordinates are (49.72°N, 73.94°W), (48.93°N, 73.82°W), (48.29°N, 73.87°W) and (47.62°N, 73.94°W), respectively. The approximate distances between the stations D-E, E-F and F-G are 87, 64 and 74 km, respectively. The VLF receivers installed at the four stations were identical and a crossed vertical loop antenna was used at each

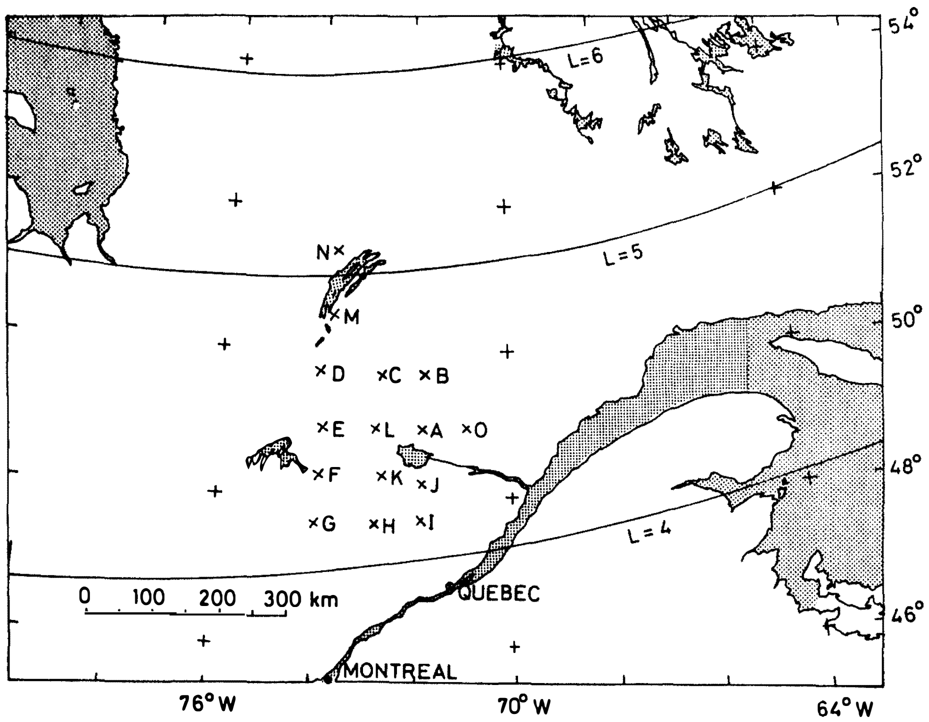

Fig. 1. The map showing the location of the observation sites. For the first half period of the experiment, receivers were installed at 12 points from A to L, and in the later period receivers were installed at M, N, D, E, F, G and O.

station. The VLF signals of whistlers were amplified and mixed with a 10 kHz reference signal and recorded on magnetic tapes at the four stations. The bandwidth of the VLF data was limited to 0–7 kHz.

Prior to the detailed analysis we converted the VLF data which had been recorded on analog tapes, to digital data in order to carry out an accurate comparison of wave intensity between the stations. In digitizing the data, we used a 25 kHz sampling clock which was made from the 10 kHz reference signal recorded on one of the tracks simultaneously with whistlers. The analysis was performed by a 1024-point fast Fourier transform (FFT). Calculations were made at each 10 ms by shifting the time window. Two Fourier components of the magnetic field (H_x, H_y) averaged for 30 ms were squared and added together so as to reduce the error due to wave polarization as much as possible.

The accuracy of the clocks used in the field operation was about 90 ms/day and not sufficient as a reference for the present analysis. Hence, we used atmospherics in order to correct the clocks. The accuracy of time in the analysis was about 0.25 ms which corresponds to the propagation time of atmospherics between the stations.

Examples of the dynamic spectrum of the multi-path whistlers observed at the stations D, E, F and G at 1501 : 03 UT on July 23, 1979 are given in Fig. 2. The slight difference of the recording gain inherent in each receiver systems was corrected in the course of the digital processing. The receivers adjust the recording gain according

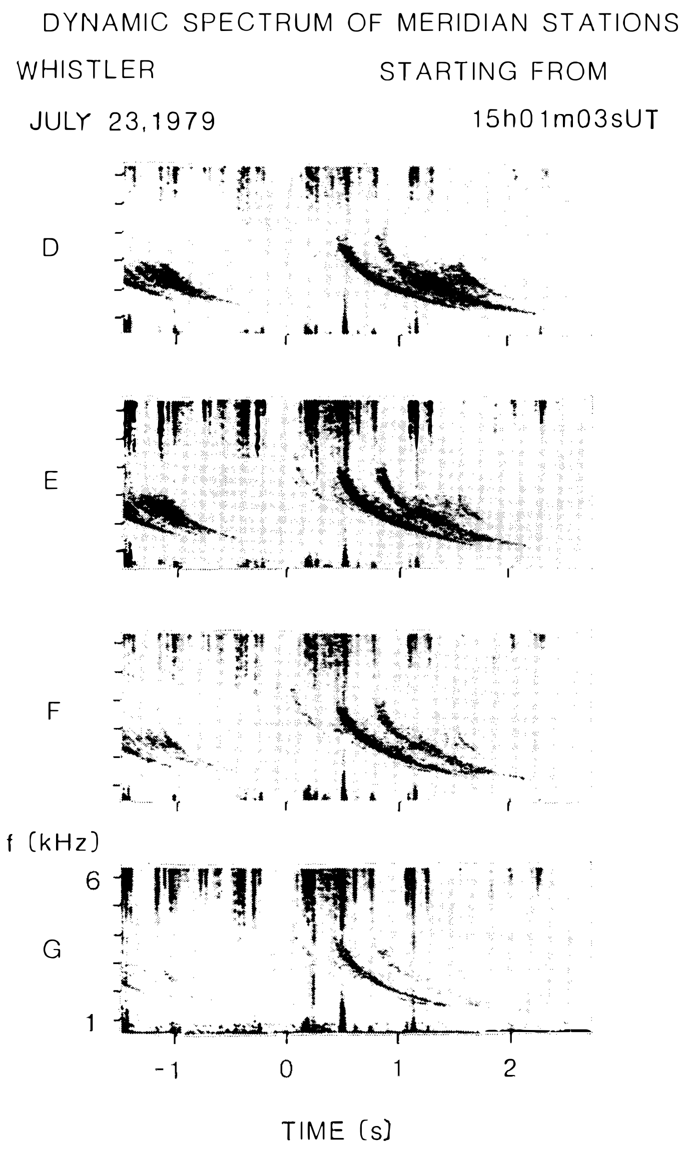

Fig. 2. The f-t dynamic spectrum of the whistler simultaneously observed at four stations near 1501 : 03 UT on July 23, 1979. Note different intensities of whistler traces between the four panels.

to the signal intensity through the AGC circuit by 9.0 dB steps. The recording gains at stations E and G were lower than those at stations D and F by 9.0 dB when the whistlers shown in Fig. 2 were being received. This was also corrected in the digital processing. The intense spherics were sometimes saturated and we could not make a comparison of their intensities between the stations, however, the intensities of all the whistlers were below the saturation level and we could make an accurate comparison. Although, it seems that the intensity of the whistlers peaks at the stations D or E in most cases, there was a slight difference between them, namely the whistlers arriving earlier at ground stations tended to have maximum intensities at station E, while those coming later showed maximum intensity at the northernmost station D. In order to make this point clear, the display shown in Fig. 3 is produced, where the characters D, E, F and G indicate the station at which the wave intensity in each frequency-time cell (Δt=10 ms, Δf=24.5 Hz) is maximum. In this paper, we shall call this method the multi-station intensity comparison (MSIC) method.

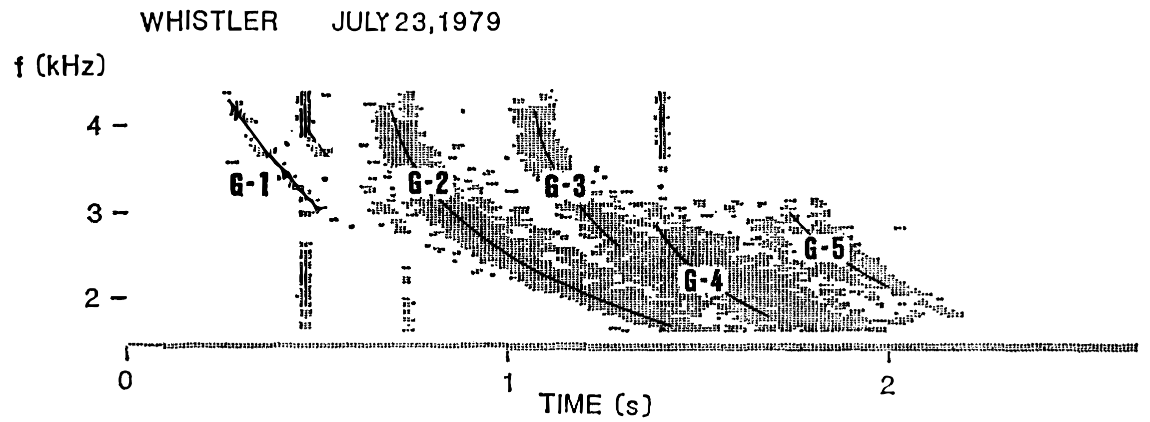

Fig. 3. The display of whistlers received at the meridian stations (D, E, F and G) indicating where the wave intensity is strongest. Stations are represented by letters in the dynamic spectrum.

There exist several whistler traces in this display. We divided them roughly into five groups, although further fine-structures in the individual groups of whistlers seem to exist. These groups are labeled as G-1, G-2, G-3, G-4 and G-5 as shown in the figure. The trace G-1 is rather weak and contains the characters D, E, F and G equally. The traces G-2 and G-3 consist mostly of the character E, while the most part of G-4 and G-5 contain the character D. This means that the whistlers G-2 and G-3 are most intense at station E, and G-4 and G-5 at the northernmost station D, as was previously mentioned. Noted that the whistler trace designated as G-3 overlapped with G-4 in the frequency range below 3 kHz.

According to the propagation theory of whistlers, the propagation time of a whistler is determined by several parameters such as electron density, magnetic field strength along the duct and length of the duct itself. It can be said that within the plasmasphere, a whistler which is excited by given sferics propagates faster through a duct in a lower latitude than in a higher latitude because the electron density in the plasmasphere decreases so slowly with the equatorial distance that the path length increase with the distance dominates to make the traveling time longer. The transition of the location from lower to higher latitudes where wave intensity is a maximum seen in Fig. 3 is consistent with that interpretation.

3. Path Locations Drived from the Wave Intensity and Nose Frequency

Wave intensities of the whistlers shown in Fig. 2 are displayed in Fig. 4 for frequencies 3.4 kHz and 2.2 kHz. The vertical axis corresponds to the distance along the meridian, while the horizontal axis corresponds to time. Intensities are digitized at 2.5 dB steps and represented by the darkness of the letters. The intensity distribution between the two neighboring stations is obtained by the linear interpolation. In the upper panel showing the intensity at 3.4 kHz, there are three whistlers G-1, G-2 and G-3, while in the lower panel showing the intensity at 2.2 kHz, four whistlers G-1, G-2, G-4, G-5 are noted. Also in this figure crosses indicate the locations of the ionospheric foot of the duct along which whistler propagated. This will be discussed in a later section.

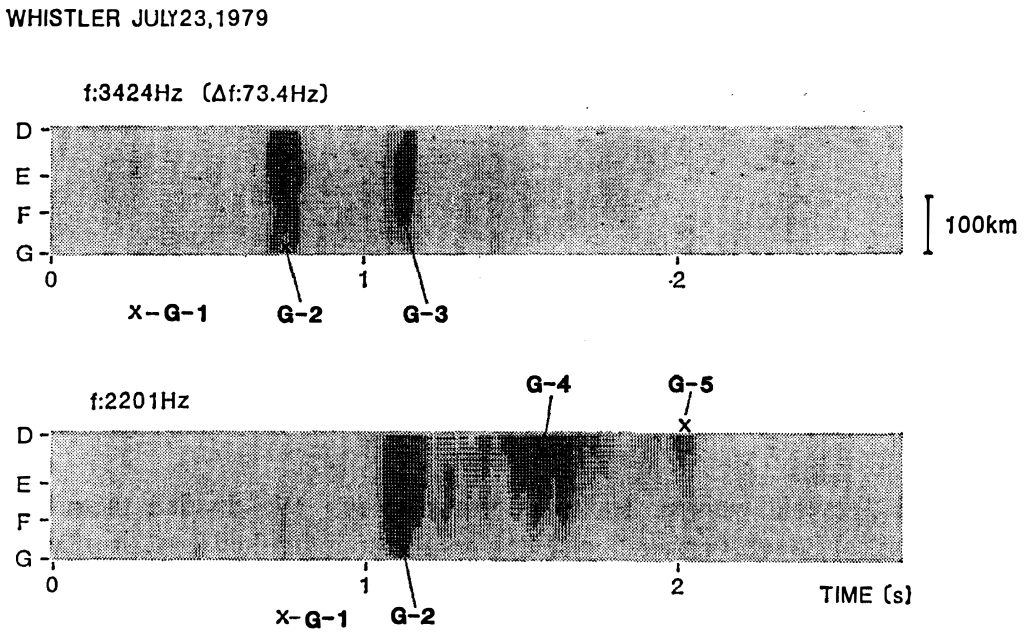

Fig. 4. Meridian display of VLF wave intensities showing the time-variation of the intensity distribution obtained for the whistlers shown in Fig. 2. The positions of duct determined by nose frequency analysis are indicated by crosses.

The whistler G-1 is rather weak but shows a slight peak in intensity around E at 3.4 kHz, and around F and G at 2.2 kHz. The whistler G-2 is intense at both frequencies 2.2 and 3.4 kHz and the intensity maxima are located around the stations E and F. The whistler G-3 has an intensity peak around station E, and seems to overlap with another group of whistler G-4 in the frequency range below 3 kHz. Since the intensity of whistler G-4 seems to be greater than that of G-3 at 2.2 kHz as judged from the intensity of G-3 at higher frequencies where G-3 and G-4 are well separated, the intensity peak seen around station D can be considered to belong to the whistler

G-4. The intensity peak of G-5 seems to be located further northward than station D. As can be seen from the lower panel of Fig. 4, a whistler trace which appear at later time shows its peak intensity at higher latitude.

We can naturally expect whistlers to have their intensity peak almost just below the wave exit region. In this regard, we compared the location of intensity peak derived from MSIC method and the whistler propagation path obtained by the Q-analysis (DOWDEN and ALLCOCK, 1971) which enables us to infer the nose frequency and its propagation time from whistler traces which do not show the nose. Using the well-known relation $f_n=0.38\, f_{Heq}$ (where f_n is the nose frequency and f_{Heq} is the equatorial gyrofrequency of the dipole magnetic field) the magnetospheric propagation paths of the whistlers are found to be $L=3.9, 4.2, 4.3, 4.6, 4.7$ for groups G-1 to G-5, respectively. Although the traces of the whistlers are not necessarily well defined, we have specified their profiles as represented by the solid lines in Fig. 3. The possible errors due to the finite width of whistler traces are 0.02 in L-value. The L-values thus obtained are indicated by the crosses in Fig. 4. As can be seen in this figure, the locations of the crosses show a tendency similar to that of the intensity peak, namely a whistler which appears at a later time shows a path location at a higher latitude. However, they have a systematic offset of about 100 km toward lower latitudes from the latitude of the peak intensity. Another discrepancy has been reported by RYCROFT *et al.* (1975) and MATTHEWS *et al.* (1979), but in contrast to the present results, their results show a shift toward higher latitudes than the wave exit region inferred from direction finding observations.

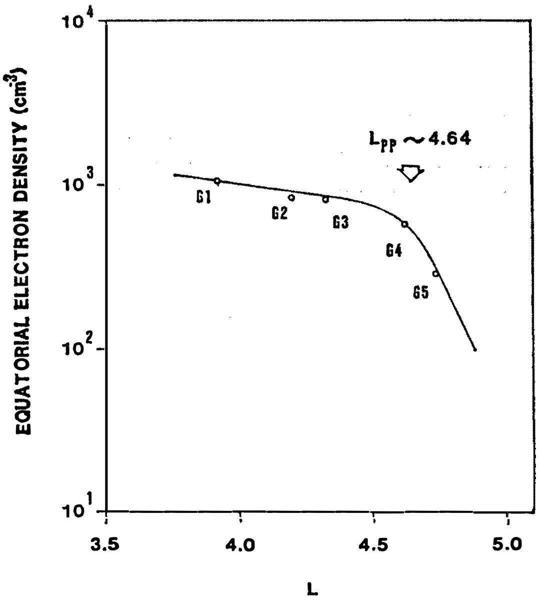

Fig. 5. The equatorial electron density inferred from the whistlers shown in Fig. 2. Ducts were located around the inner edge of the plasmapause. The arrow shows the estimated position of the plasmapause according to the formula given by CARPENTER *and* PARK *(1973).*

The equatorial electron density is obtained adopting PARK's DE-1 model (PARK, 1972) and this is represented in Fig. 5. The value ranges from 450 to 120 cm^{-3}. As can be seen in this figure, the received whistlers have propagated along the ducts located around the outer edge of the plasmasphere.

4. Attenuation Rate of Whistlers with Distance

Not much attention has been paid to the size and the shape of the wave exit region in the past, but this becomes a quite important problem when we apply the DF technique. If the size of the wave exit region is much larger than the wave length the DF

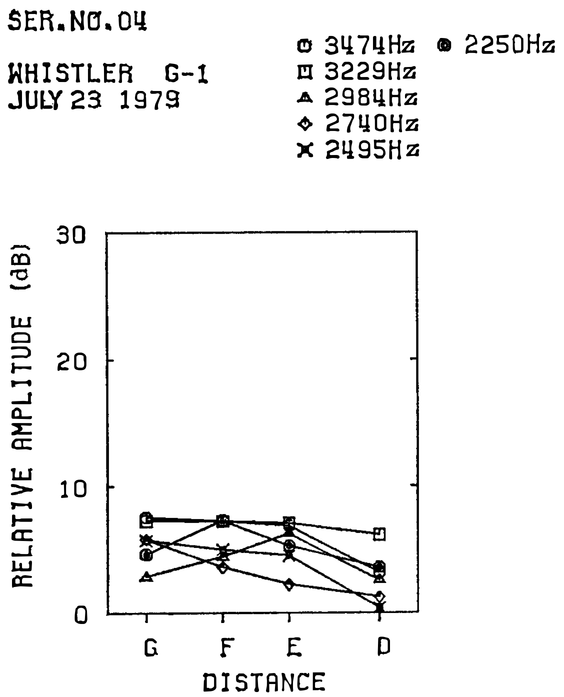

Fig. 6a.

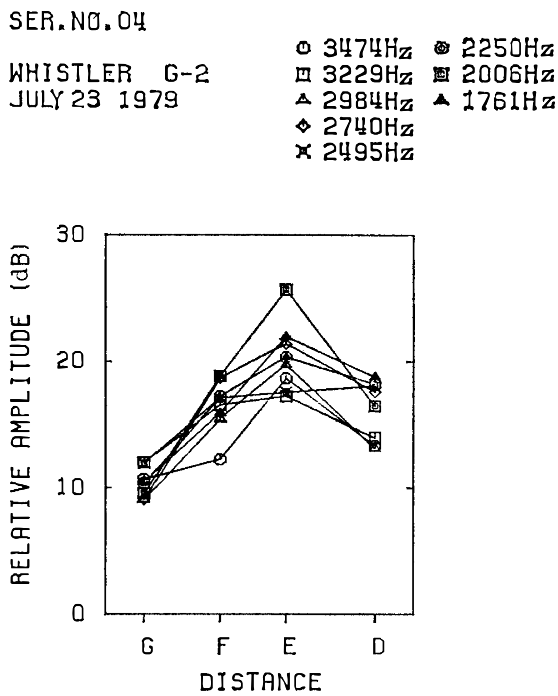

Fig. 6b.

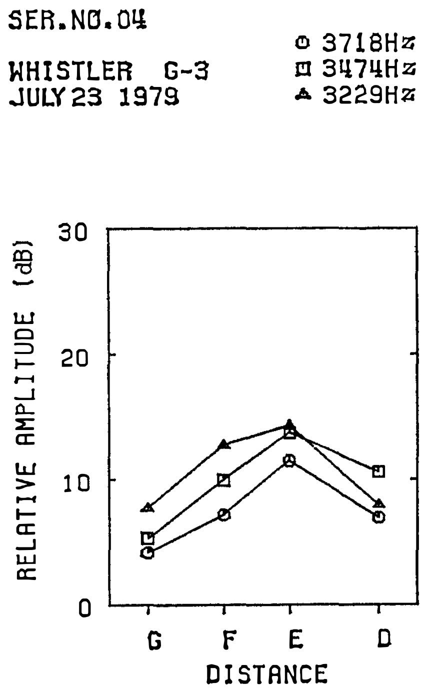

Fig. 6c.

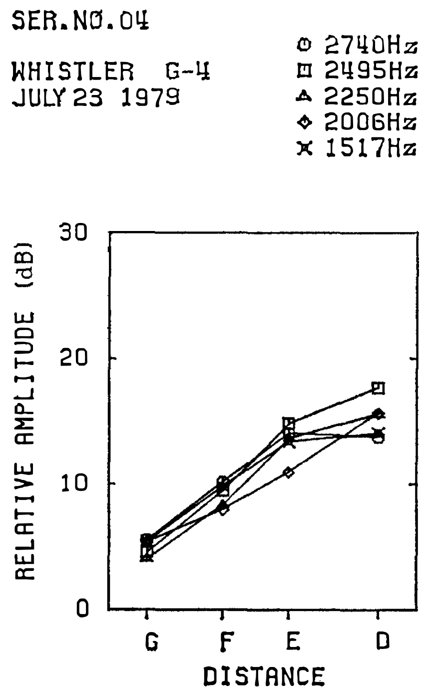

Fig. 6d.

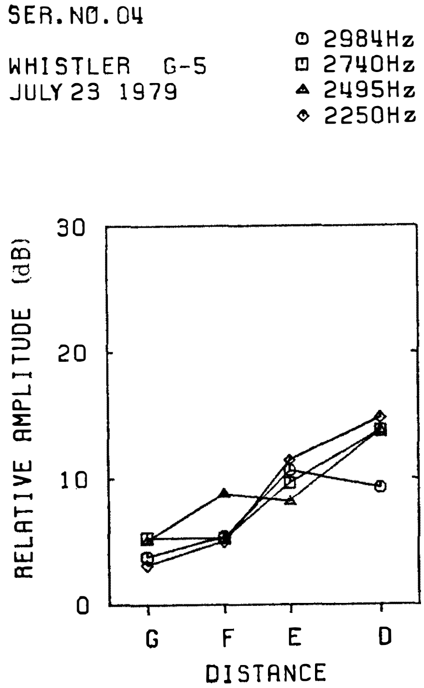

Fig. 6e.

Fig. 6. The intensity distributions of whistler G-1 to G-5, respectively. Distribution was obtained at several frequencies along the whistler trace.

method will yield erroneous bearings. The intensity distribution obtained from the observations at multi-stations on the ground gives us indication of the size and shape of the whistler exit region at the ionosphere. The whistlers G-1 to G-5 in Fig. 3 are examined from this point of view. The magnitude of the Fourier components are monitored along each whistler trace. The bandwidth of the analysis is 73.4 Hz. The result is presented in Figs. 6a to 6e. As is seen in Figs. 6b and 6c the spatial distribution of the whistler amplitude shows a well defined peak. This indicates a relatively small exit region as well as high spatial attenuation gradient of the wave intensity. The attenuation gradient is roughly 6 dB/100 km except for the case of Fig. 6a which shows a relatively low attenuation. In the cases displayed in Figs. 6d and 6e, the intensity peak seems to be located to the north of station D, that is, beyond the station chain.

In order to reduce the error due to noise, the digitized intensity of the traces of six multi-path whistlers are summed up on the same *f-t* plane and averaged spatial profiles are obtained, where the starting time of each whistler, listed in Table 1, is taken as a common time origin. Significant changes in the intensity distribution were not recognized among the whistlers listed in Table 1. The spatial distribution of the averaged intensity at several frequencies of each whistler group are given in Figs.

Table 1. List of the starting times of the whistlers used in the analysis.

No.	Starting time	No.	Starting time
1	1432:14.3 UT	4	1501:03.0 UT
2	1447:22.3	5	1501:19.1
3	1447:26.2	6	1517:26.0

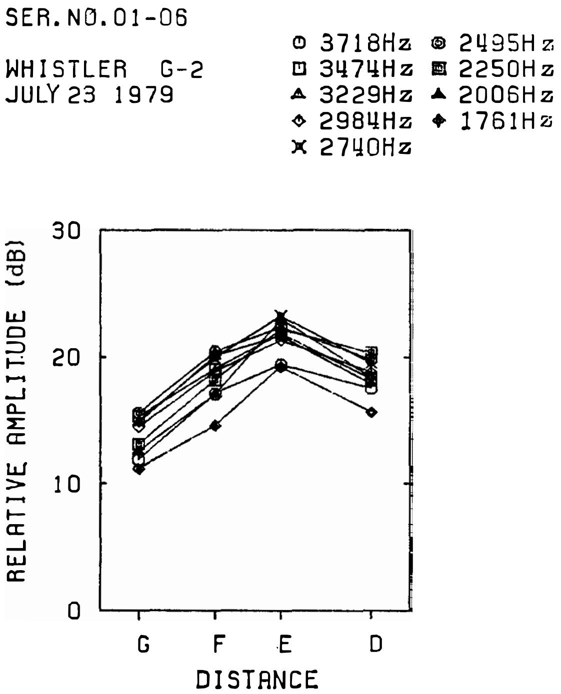

Fig. 7a.

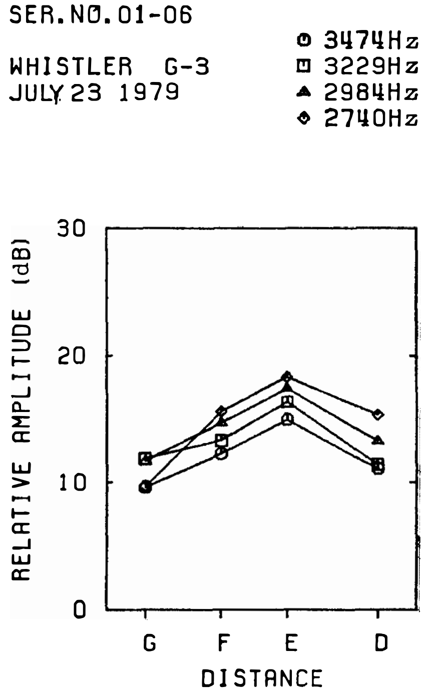

Fig. 7b.

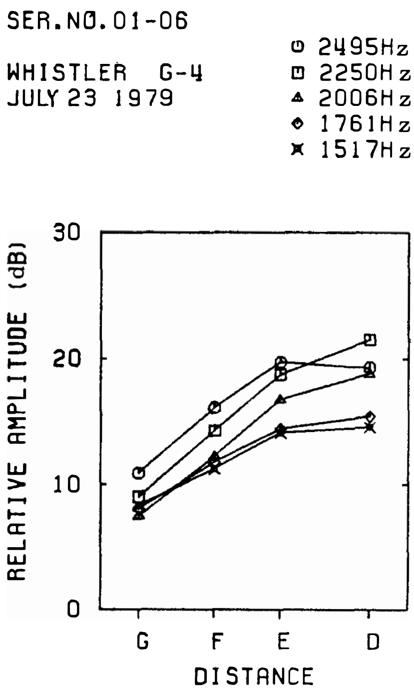

Fig. 7c.

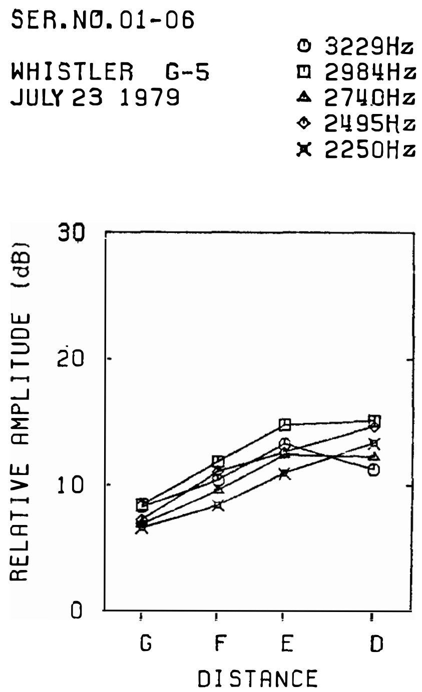

Fig. 7d.

Fig. 7. The averaged intensity distributions of four whistlers. Designations of whistlers are same as shown in Fig. 3.

7a to 7d. The designation of the whistler groups is the same as that in Fig. 3. The distribution for the whistler G-1 was not obtained since the intensity was too weak to perform the analysis. The general tendency seen from the curves in Figs. 7a to

7d is similar to what has been derived from the analysis of a particular whistler received around 1501: 03 UT.

We looked for systematic variations of the attenuation gradient with frequency, but no relationship between the attenuation gradient and the wave frequency could not be found in the cases given in Figs. 6a to 6e nor in Figs. 7a to 7d. The attenuation gradient with the distance is about 6 dB/100 km in the vicinity of the intensity maximum for most cases investigated in this study. It is interesting to note that the wave intensity distribution reveals no systematic dependence on frequency although the lowest frequency (1.5 kHz) wave has a wave length more than twice of that of the highest frequency (3.7 kHz) wave.

5. Discussion

Through the whistler observation carried out at multiple stations following can be summarized:

1. An attenuation gradient of the whistlers as high as 6 dB/100 km is obtained and no systematic dependence of the gradient on the wave frequency is found in the frequency range of 1.5 to 3.7 kHz.
2. Owing to this high attenuation gradient, we were able to determine the location of the wave exit region by the MSIC method (Multi-Station Intensity Comparison method) despite the closeness of the stations (about 70 km).
3. Among the whistler traces excited simultaneously by the same sferics, the ones which are received later show intensity maxima at a higher latitude.
4. The intensity maxima derived from the MSIC method are located systematically at about 100 km towards a higher latitude than the ionospheric foot locations of the ducts obtained by the nose frequency analysis.

The spatial attenuation gradient of whistlers observed at four ground stations was approximately 6 dB per 100 km. This value is the same as that obtained for the Siple signals and chorus emissions (TSURUDA *et al.*, 1982), and considerably higher than what would be expected from the coupling theory between whistler mode and the earth-ionosphere cavity mode (WALKER, 1974). He gave 1.2 dB per 100 km as a typical spatial attenuation gradient for whistlers. With the high spatial attenuation of whistlers obtained in our experiments, whistlers cannot propagate such a long distance. Hence, our results conflict with the past experiments which demonstrated a long distance propagation of whistlers in the earth-ionosphere cavity. One possible explanation for this discrepancy is that the high attenuation gradient obtained in the present experiment is due to the closeness of the station network to the whistler exit region. And at greater distances the attenuation gradient would become smaller as found from past experiments. The case presented in Fig. 6a might represent the low attenuation at a large distance from the exit region. Recently, NAGANO *et al.* (1981, private communication) calculated the coupling of downcoming whistler waves with a Gaussian amplitude profile to the cavity mode and obtained high spatial attenuation near the exit region. These calculations would help us in understanding the coupling process and also in planning a future campaign with a larger spatial span.

The whistler exit region inferred from amplitude peak on the ground was about 100 km north of the ionospheric foot of its propagation path derived from the nose-frequency analysis. A similar difference has been noted for the exit region deduced from the direction finding experiments. SEELY (1977) studied the relationship between the whistler nose frequency and the equatorial path latitude using the IGRF model of the geomagnetic field, and found that the foot of the magnetic field near Roberval calculated by the IGRF model is displaced toward the high-latitude by 100 km from that calculated by the dipole model. His result seems to explain the northward deviation of the whistler exit region for the present experiment since the path latitude was determined by the dipole magnetic field in the nose-frequency analysis. According to BERNHARDT and PARK (1977), the altitude of the end point of whistler duct is not lower than 1000 km in the summer hemisphere. Hence we have to consider that a whistler propagates downward to the lower ionosphere almost along the geomagnetic field line after leaving the duct at an altitude of over 1000 km. The horizontal gradient of the electron density in the topside ionosphere will cause the deflection of the whistler ray toward low latitude side of the foot of duct (RYCROFT *et al.*, 1975; THOMSON and DOWDEN, 1978) and the modification of the dipole field due to the ring current would result in the low latitude shift of the whistler exit region from the foot of the field line determined from the nose frequency by assuming a pure dipole magnetic field (SAGREDO and BULLOUGH, 1973). Since the results from the present experiment gave a deviation of the exit region in the opposite sense to that expected from the discussion given above, these mechanisms may not have been dominant in our case.

Acknowledgments

We wish to thank Prof. A. NISHIDA, Drs. K. MAEZAWA and T. TERASAWA for their support throughout the field campaign and valuable comments and discussions. We also thank Drs. K. HAYASHI and H. FUKUNISHI for very useful discussions and comments. We greatly appreciate for the cooperation in this experiment and the useful discussions from the planning stage of the experiment with Profs. R. A. HELLIWELL, J. P. KATSUFRAKIS and D. L. CARPENTER.

References

BERNHARDT, P. A. and PARK, C. G. (1977): Protonospheric-ionospheric modeling of VLF ducts. J. Geophys. Res., **82**, 5222–5230.

CARPENTER, D. L. (1980): Fast fluctuations in the arrival bearing of magnetospherically propagation signals from the Siple, Antarctica, VLF transmitter. J. Geophys. Res., **85**, 4157–4166.

DOWDEN, R. L. and ALLCOCK, G. McK. (1971): Determination of nose frequency of non-nose whistlers. J. Atmos. Terr. Phys., **33**, 1125–1129.

LEAVITT, M. K. (1974): Initial results from a tracking receiver direction finder for whistler mode signals. J. Geophys. Res., **83**, 1601–1610.

MATTHEWS, J. P., SMITH, A. J. and SMITH, I. D. (1979): A remote unmanned ELF/VLF goniometer receiver in Antarctica. Planet. Space Sci., **27**, 1391–1001.

OKADA, T., IWAI, A. and HAYAKAWA, M. (1977): The measurement of the incident and azimuthal angles and the polarization of whistlers at low latitudes. Planet. Space Sci., **25**, 233–241.

PARK, C. G. (1972): Method of determining electron concentrations in the magnetosphere from nose whistlers. Tech. Rep. Radiosci. Lab., Stanford Univ., No. **3454**-1, 100 p.

Rycroft, M. J., Jarvis, M. J. and Strangeways, H. J. (1975): Determination by triangulation of the regions where whistlers emerge from the ionosphere. ESRO Spec. Publ., **107**, 225.

Sagredo, J. L. and Bullough, K. (1972): The effect of the ring current on whistler propagation in the magnetosphere. Planet. Space Sci., **20**, 731–746.

Sagredo, J. L. and Bullough, K. (1973): VLF goniometer observations at Halley Bay, Antarctica. II. Magnetospheric structure deduced from whistler observations. Planet. Space Sci., **21**, 913–923.

Seely, N. T. (1977): Whistler propagation in a distorted quiet-time magnetosphere. Tech. Rep. Radiosci. Lab., Stanford Univ., No. **3472**-1,

Thomson, R. J. and Dowden, R. L. (1978): Ionospheric whistler propagation. J. Atmos. Terr. Phys., **40**, 215–221.

Tsuruda, K. and Hayashi, K. (1975): Direction finding technique for eliptically polarized VLF electromagnetic waves and its application to the low-latitude whistlers. J. Atmos. Terr. Phys., **37**, 1193–1202.

Tsuruda, K. and Ikeda, M. (1979): Comparison of three different types of VLF direction-finding techniques. J. Geophys. Res., **84**, 5325–5332.

Tsuruda, K., Machida, S., Terasawa, T., Nishida, A. and Maezawa, K. (1982): High spatial attenuation rate of the Siple transmitter signal and natural VLF chorus observed at a ground-based chain stations near Roberval, Quebec. J. Geophys. Res., **87**, 742–750.

Walker, A. D. M. (1974): Excitation of earth-ionosphere waveguide by downcoming whistlers II. Propagation in the magnetic meridian. Proc. R. Soc. London, A, **340**, 375–393.

(Received November 30, 1981; Revised manuscript received March 25, 1982)